Spleen volume-based non-invasive tool for predicting hepatic decompensation in people with compensated cirrhosis (CHESS1701)

Authors

Qian Yu, Chuanjun Xu, Qinyi Li, Zhimin Ding, Yan Lv, Chuan Liu, Yifei Huang, Jiaying Zhou, Shan Huang, Cong Xia, Xiangpan Meng, Chunqiang Lu, Yuefeng Li, Tianyu Tang, Yuancheng Wang, Yang Song, Xiaolong Qi, Jing Ye, Shenghong Ju

Correspondence

jsh@seu.edu.cn (S. Ju).

Graphical abstract

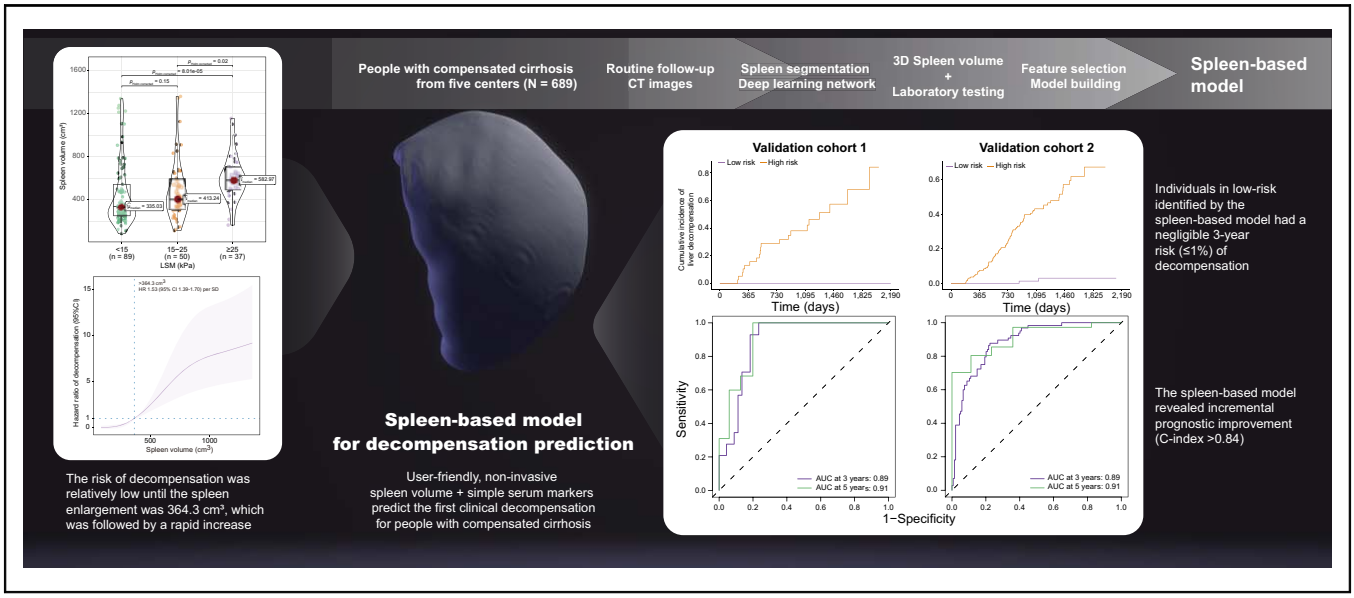

Highlights

- Spleen volume is a predictor for decompensation by rapid risk increasement after spleen volume >364 cm^3.
- The spleen-based model revealed incremental prognostic improvement (C-index >0.84).
- Low-risk patients identified by the spleen-based model had a negligible 3-year risk (≤1%) of decompensation.

Lay summary

People with compensated cirrhosis with larger spleen volume would have a higher risk of decompensation. We developed a spleen-based model and validated it in external validation cohorts. The proposed model might help predict hepatic decompensation in people with compensated cirrhosis when invasive tools are unavailable.

https://doi.org/10.1016/j.jhepr.2022.100575

Research article

JHEP|Reports

Spleen volume-based non-invasive tool for predicting hepatic decompensation in people with compensated cirrhosis (CHESS1701)

Qian Yu,[1] Chuanjun Xu,[2] Qinyi Li,[3] Zhimin Ding,[4] Yan Lv,[5] Chuan Liu,[6] Yifei Huang,[7] Jiaying Zhou,[1] Shan Huang,[1] Cong Xia,[1] Xiangpan Meng,[1] Chunqiang Lu,[1] Yuefeng Li,[8] Tianyu Tang,[1] Yuancheng Wang,[1] Yang Song,[9] Xiaolong Qi,[6] Jing Ye,[5] Shenghong Ju[1,*]

[1]*Department of Radiology, Zhongda Hospital, School of Medicine, Southeast University, Nanjing, China;* [2]*Department of Radiology, The Second Hospital of Nanjing, Nanjing University of Chinese Medicine, Nanjing, China;* [3]*Department of Radiology, The Affiliated Third Hospital of Jiangsu University, Zhenjiang, China;* [4]*Department of Radiology, Yijishan Hospital of Wannan Medical College, Wuhu, China;* [5]*Department of Medical Imaging, Subei People's Hospital, Medical School of Yangzhou University, Yangzhou, China;* [6]*Center of Portal Hypertension, Department of Radiology, Zhongda Hospital, School of Medicine, Southeast University, Nanjing, China;* [7]*CHESS Center, Institute of Portal Hypertension, The First Hospital of Lanzhou University, Lanzhou, China*
[8]*Department of Radiology, The Affiliated Hospital of Jiangsu University, Zhenjiang, China;* [9]*MR Scientific Marketing, Siemens Healthineers Ltd., Shanghai, China*

JHEP Reports **2022.** https://doi.org/10.1016/j.jhepr.2022.100575

Background & Aims: Non-invasive stratification of the liver decompensation risk remains unmet in people with compensated cirrhosis. This study aimed to develop a non-invasive tool (NIT) to predict hepatic decompensation.
Methods: This retrospective study recruited 689 people with compensated cirrhosis (median age, 54 years; 441 men) from 5 centres from January 2016 to June 2020. Baseline abdominal computed tomography (CT), clinical features, and liver stiffness were collected, and then the first decompensation was registered during the follow-up. The spleen-based model was designed for predicting decompensation based on a deep learning segmentation network to generate the spleen volume and least absolute shrinkage and selection operator (LASSO)-Cox. The spleen-based model was trained on the training cohort of 282 individuals (Institutions I–III) and was validated in 2 external validation cohorts (97 and 310 individuals from Institutions IV and V, respectively) and compared with the conventional serum-based models and the Baveno VII criteria.
Results: The decompensation rate at 3 years was 23%, with a 37.6-month median (IQR 21.1–52.1 months) follow-up. The proposed model showed good performance in predicting decompensation (C-index ≥0.84) and outperformed the serum-based models (C-index comparison test p <0.05) in both the training and validation cohorts. The hazard ratio (HR) for decompensation in individuals with high risk was 7.3 (95% CI 4.2–12.8) in the training and 5.8 (95% CI 3.9–8.6) in the validation (log-rank test, p <0.05) cohorts. The low-risk group had a negligible 3-year decompensation risk (≤1%), and the model had a competitive performance compared with the Baveno VII criteria.
Conclusions: This spleen-based model provides a non-invasive and user-friendly method to help predict decompensation in people with compensated cirrhosis in diverse healthcare settings where liver stiffness is not available.
Lay summary: People with compensated cirrhosis with larger spleen volume would have a higher risk of decompensation. We developed a spleen-based model and validated it in external validation cohorts. The proposed model might help predict hepatic decompensation in people with compensated cirrhosis when invasive tools are unavailable.

Introduction

In the natural history of chronic liver disease, clinical decompensation (ascites, variceal bleeding, and encephalopathy) is recognised as a prognostic indicator because mortality is almost unalterably preceded by decompensation.[1,2] People with compensated cirrhosis who are at a high decompensation risk need to be promptly identified for intensive monitoring and intervention to avoid the progression to decompensation.[1,3] Notably, liver stiffness measurement (LSM) and platelet (PLT) count were proposed to screen clinically significant portal hypertension (CSPH) and high-risk varices, indirectly providing evidence for decompensation risk stratification.[4] However, in non-specialised settings and across diverse healthcare systems where hepatic venous pressure gradient (HVPG, the gold standard for CSPH) and LSM are unavailable, the use of robust prognostic non-invasive tools (NITs) using common variables to

Keywords: Cirrhosis; Decompensation; CT; Deep learning; Spleen; Splenomegaly; CHESS1701.
Received 18 May 2022; received in revised form 14 July 2022; accepted 16 August 2022; available online 27 August 2022
* Corresponding author. Address: Department of Radiology, Zhongda Hospital, School of Medicine, Southeast University, Nanjing, China. Tel.: +86-83272121
E-mail address: jsh@seu.edu.cn (S. Ju).

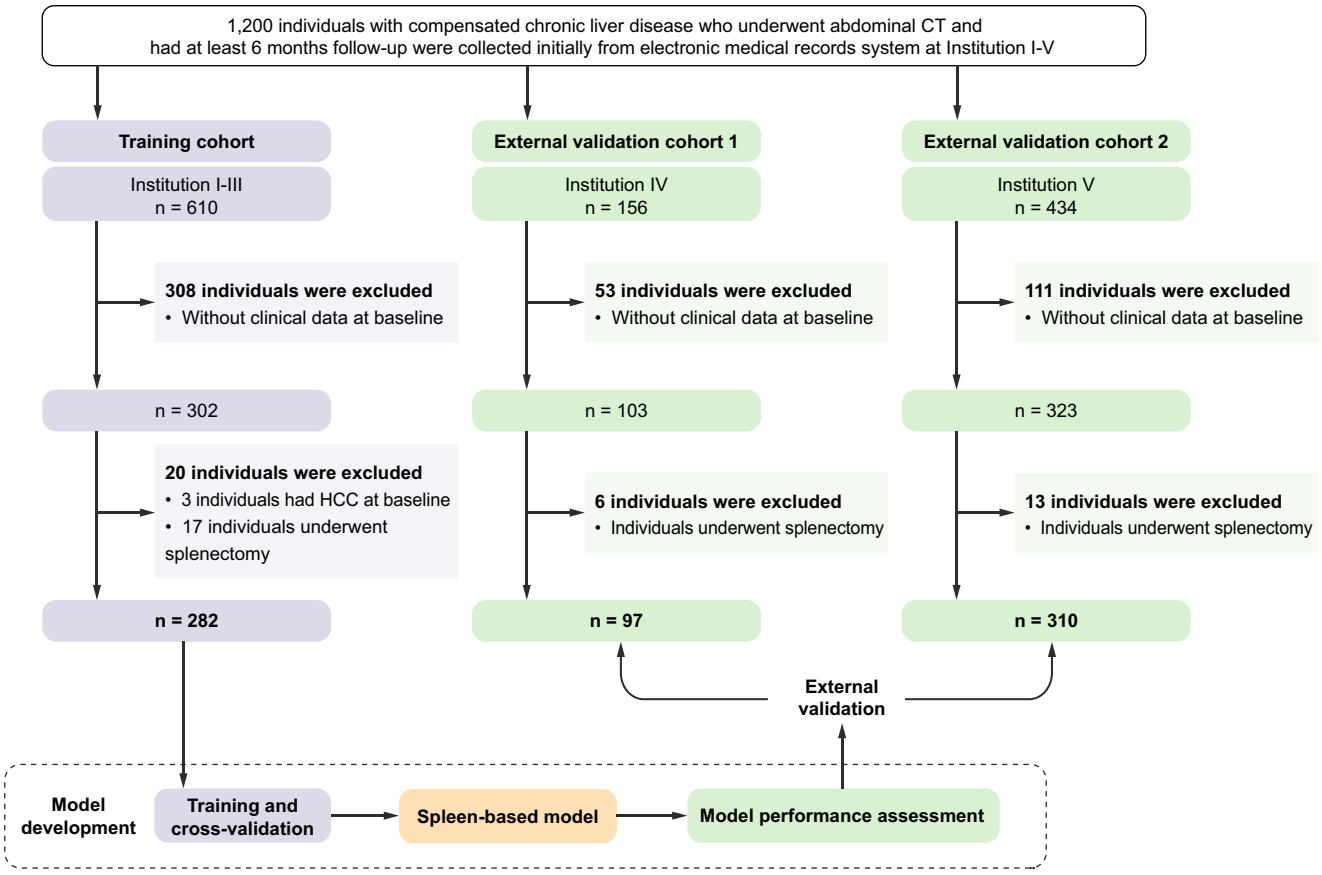

Fig. 1. Flowchart of patient inclusion. CT, computed tomography; HCC, hepatocellular carcinoma.

stratify the liver decompensation risk remains as an unmet need in people with compensated cirrhosis.

Spleen morphology has been considered in the diagnosis and prediction of complications of liver cirrhosis for decades.[5–7] Structural changes in the spleen occur in portal hypertension owing to not only passive congestion of the spleen, but also angiogenesis and fibrogenesis.[8] Initially, spleen diameter, as determined by ultrasound, increased the accuracy of NITs based on LSM for portal hypertension, varices, and decompensation.[6,7,9–13] The longitudinal spleen axis on ultrasound has always been analysed in previous studies.[5–7] However, this measurement is associated with errors owing to the heterogeneity in ultrasound measurements and the spatial transformation of splenomegaly.

Previous studies adopted a 2-dimensional (2D) spleen diameter from ultrasound to build a predictive model with clinical characteristics for decompensation, which might reduce the significance of spleen in decompensation and the performance of the model. Advancements in deep learning techniques have made it possible to obtain a quantitative 3-dimensional (3D) volumetric analysis of the spleen,[14,15] providing a basis for potential predictive models based on spleen characteristics. Spleen volume has been recently considered larger in the decompensated population than in compensated individuals,[10,14,15] which is considered a risk factor for decompensation.[11,12]

Machine learning has shown potential for non-invasively predicting cirrhosis-related events,[16–18] such as by analysing clinical and laboratory data. Machine learning is a branch of data science that uses computational modelling to learn from data. These models have the potential to improve the risk stratification provided by conventional clinical risk scores[18] Meanwhile, joint modelling of spleen volume and clinical variables can reveal the effect of the spleen on clinical features in predicting decompensation. Finally, studies on spleen volume-based prediction models for decompensation have been limited by standard statistical analyses, the absence of external validation, and/or the absence of comparisons with conventional clinical risk assessment scores.[11,12,19]

Therefore, we hypothesised that spleen volume would better drive a predictive model for people with cirrhosis at a high risk of decompensation. This study aimed to build a user-friendly non-invasive model that combines spleen volume and simple serum markers to predict the first clinical decompensation in people with compensated cirrhosis and compare it with existing clinical models.

Patients and methods

Study participants

This is an investigator-initiated, retrospective, multicentre cohort study that was conducted at 5 liver centres in China. Potential candidates were enrolled between January 2016 and June 2020. The local institutional review boards approved this study, and the requirements for written informed consent were waived.

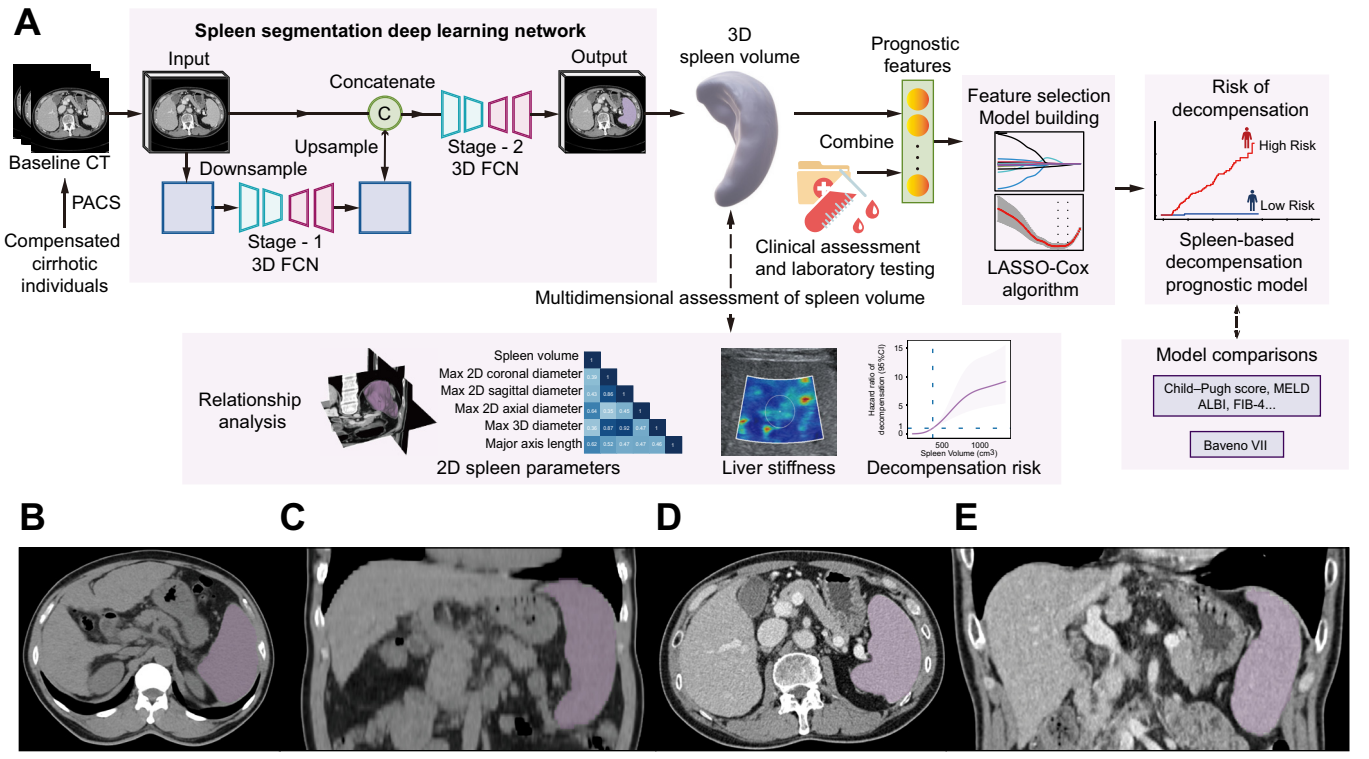

Fig. 2. Spleen segmentation examples in unenhanced CT and contrast-enhanced CT. (A) The spleen-based model development workflow. (B and C) Spleen segmentation in unenhanced axial and coronal abdominal CT of a 55-year-old man with HCV liver cirrhosis with a spleen volume of 675.4 cm^3. The patient was identified as high decompensation risk with a prognostic value of 5.0 (cut-off value 4.4). Overt ascites was diagnosed 535 days after baseline CT. (D and E) Spleen segmentation in contrast-enhanced axial and coronal abdominal CT of a 62-year-old man with HCV liver cirrhosis with a spleen volume of 429.6 cm^3. The patient was identified as high decompensation risk with a prognostic value of 4.9. Variceal bleeding happened 505 days after baseline CT. 2D, 2-dimensional; 3D, 3-dimensional; ALBI, albumin–bilirubin; CT, computed tomography; FCN, fully convolutional network; FIB-4, Fibrosis-4; MELD, model for end-stage liver disease; PACS, picture archiving and communication systems.

The inclusion criteria for patients were as follows: (1) adults (aged 18–75 years); (2) with confirmed cirrhosis diagnosed by laboratory tests, imaging methods, physical examination findings, or biopsy[20] (see detailed diagnostic criteria in the Supplementary Methods 1.1); (3) who had abdominal computed tomography (CT) in a routine cirrhosis assessment; (4) did not have present or past decompensation (ascites, variceal bleeding, or hepatic encephalopathy)[1]; (5) did not have decompensation within the 6 months after baseline CT; and (6) with at least 6 months of follow-up after the CT scan.[21]

The exclusion criteria were as follows: (1) individuals who previously underwent any surgical procedures of the liver or spleen (*e.g.* transjugular intrahepatic portosystemic shunt [TIPS], liver transplantation, splenectomy, or partial splenic embolisation); (2) had hepatocellular carcinoma; (3) had portal vein thrombosis; and (4) with no available clinical data at baseline.

A total of 1,200 patient profiles were collected initially from 5 different centres (Fig. 1). After the patient-by-patient inclusion, 689 individuals were enrolled in this study. Patients were divided into 3 cohorts: (1) training cohort (n = 282 from Institutions I, II, and III) for model training and variable selection; (2) external validation cohort 1 from Institution IV (n = 97); and (3) external validation cohort 2 from Institution V (n = 310) for model testing. There is no overlap between each cohort.

Liver-related events and follow-up

The primary endpoint was classic clinical decompensation, which was defined as overt ascites, variceal haemorrhage, or hepatic encephalopathy.[1] Variceal haemorrhage and hepatic encephalopathy were labelled acute decompensation and would be further analysed.[2] The details of the definitions are shown in Supplementary Methods 1.2. The follow-up started at the time of the baseline CT scan, which was performed while 1 patient was on a routine follow-up schedule, starting in January 2016. Patients were followed up until the first meeting of the primary endpoint, until death, or until the end of December 2021. The last follow-up evaluation date and the last status were registered for patients who were no longer available for follow-up.

Outpatient and inpatient digital medical records were extracted and reviewed in each centre for follow-up by board-certified gastroenterologists. In accordance with medical insurance policies and clinician requirements, patients were regularly followed up at least every 6 months for cirrhosis assessment and for (1) antiviral therapy (or individuals who needed medications for other types of cirrhosis), (2) blood tests, (3) variceal screening, or (4) routine imaging examinations (ultrasound, CT, or magnetic resonance imaging [MRI]). Ascites was screened in time using imaging methods if it was clinically suspected outside the follow-up schedule. Variceal bleeding and hepatic encephalopathy were diagnosed by an experienced clinician in a patient requiring admission.

Table 1. Baseline characteristics of cohorts.

Variables	Total (N = 689)	Training cohort (n = 282)	External Validation cohort 1 (n = 97)	External Validation cohort 2 (n = 310)
Age, years	54 (17)	56 (18)	52 (17)	54 (17)
Sex, male	441 (64)	176 (62)	64 (66)	201 (65)
Weight, kg	64 (16)	63 (15)	65.5 (18.83)	64 (10)
Height, cm*	165.2 (8.9)	161.6 (8.3)	166.4 (8.3)	166.6 (7)
ALB, g/L	39.7 (8.8)	40.1 (7.65)	42.7 (9.9)	38.1 (9.05)
TBIL, μmol/L	18 (14.36)	18.59 (15.71)	17.5 (9.15)	17.7 (15.17)
IBIL, μmol/L	11 (7.98)	11.7 (8.43)	11.65 (5.22)	10.45 (7.93)
DBIL, μmol/L	6.3 (6.3)	6.4 (6.72)	5.3 (4.5)	6.5 (7.07)
ALT, IU/L	34 (35)	36 (33)	38 (31.5)	33 (37)
AST, IU/L	34.7 (27.3)	35 (27)	35 (27.5)	32.8 (27.5)
ALP, IU/L	94 (55.72)	97 (57)	89 (46.5)	94.1 (57.7)
GGT, IU/L	57 (89.1)	63 (109)	44 (71.5)	56.8 (76.9)
CHE, U/L	5,893 (3241)	6,000 (2759)	6,646 (3248)	5,545 (3360)
BUN, mmol/L	4.79 (1.92)	4.7 (2.03)	4.85 (2.12)	4.79 (1.88)
Cr, μmol/L	66 (22)	66.3 (23.15)	69 (19.25)	64.5 (20.75)
UA, μmol/L	295.6 (132.4)	292.85 (127.6)	311 (130)	296 (136)
Hb, g/L	134 (30)	135 (30)	140 (26)	131 (31.5)
Platelets, $\times 10^9$/L	103 (76)	103 (76.75)	127 (63.5)	98 (72.5)
INR	1.14 (0.23)	1.1 (0.19)	1.2 (0.2)	1.17 (0.23)
Spleen volume, cm^3	364.3 (351.9)	354.2 (350.8)	335.9 (310.7)	385.8 (346.3)
Child–Pugh score, n (%)				
A, 5	273 (50)	109 (52)	22 (49)	142 (48)
A, 6	134 (24)	60 (29)	10 (22)	64 (22)
B, 7	78 (14)	21 (10)	9 (20)	48 (16)
B, 8	29 (5)	9 (4)	3 (7)	17 (6)
B, 9	36 (7)	9 (4)	1 (2)	26 (9)
MELD	6.72 (5.59)	5.53 (6.11)	5.64 (5.04)	7.37 (5.3)
ALBI	−2.57 (0.82)	−2.61 (0.74)	−2.88 (0.89)	−2.4 (0.82)
FIB4	3.46 (3.7)	3.24 (3.68)	3.15 (4.07)	3.75 (3.66)
ALBI-FIB4	−2.74 (1.56)	−2.83 (1.41)	−3.14 (1.76)	−2.58 (1.67)
Aetiology, n (%)				
Viral hepatitis	485 (70)	188 (67)	77 (79)	220 (71)
Alcohol	32 (5)	18 (6)	5 (5)	9 (3)
Cholestatic and autoimmune liver disease	91 (13)	34 (12)	10 (10)	47 (15)
Other	81 (12)	42 (15)	5 (5)	34 (11)

Except where indicated, data are reported by median (IQR). This model used the following variables: aetiology (viral hepatitis), aetiology (sustained virological responses), aetiology (alcohol), aetiology (cholestatic and autoimmune liver disease), ALB, TBIL, IBIL, DBIL, ALT, AST, AST/ALT, ALP, GGT, CHE/1,000, BUN, Cr, UA, Hb, platelets, INR, Child–Pugh score, MELD, ALBI, FIB-4, and ALBI-FIB-4. LASSO could resolve any potential co-linearities among these features.
ALB, albumin; ALBI, albumin–bilirubin; ALP, alkaline phosphatase; ALT, alanine aminotransferase; AST, aspartate transaminase; CHE, cholinesterase; Cr, creatinine; DBIL, direct bilirubin; FIB-4, Fibrosis-4; GGT, gamma-glutamyltransferase; Hb, haemoglobin; IBIL, indirect bilirubin; INR, international normalised ratio; LASSO, least absolute shrinkage and selection operator; MELD, model for end-stage liver disease; TBIL, total bilirubin; UA, urine albumin.
* Mean (SD).

Demographic, clinical, laboratory data, and liver stiffness

Baseline characteristics of patients were collected, including demographics (age and sex), clinical data (aetiology and sustained virological response), and laboratory data (liver function, renal function, PLT count, haemoglobin [Hb], and coagulation function) at the time of the CT scan. The Child–Pugh score, model for end-stage liver disease (MELD), albumin–bilirubin (ALBI) score, Fibrosis-4 (FIB-4), and ALBI-FIB4 score were calculated using the baseline characteristics.[4,22] A total of 176 liver stiffness measurement results (kPa) using transient elastography (FibroScan®, Echosens, Paris, France) were extracted from Institution V (validation cohort 2) within 1 week around the time of the baseline CT.

Spleen-based model development

The spleen-based model included 2 main components: automated spleen segmentation and decompensation risk prediction. The input of the model was the original abdominal CT images, and the output was the risk score of decompensations (Fig. 2A).

We first used a 2-step deep learning network to segment the spleen area on CT images automatically (Fig. 2A). The input CT images were resampled to 3-mm thickness (details of CTs in each institution are summarised in Table S1). The network was based on two 3D fully convolutional networks (FCNs) and was optimised for cirrhosis and splenomegaly. Finally, the network output of the spleen mask and the 3D spleen volume were calculated according to the segmentation.

The deep learning algorithm is described in our previous study[18] and is available online (https://github.com/vanziaa/aHVPG), and the examples of spleen segmentation are shown in Fig. 2. All segmentation results were checked (SH and JYZ, board-certified radiologists). To test the accuracy of the segmentation results, 10% (69/689) of individuals from 5 centres were selected by stratified random sampling, and 3 radiologists, who were blinded to the spleen mask generated by deep learning model, segmented the spleen in these individuals manually. The mean Dice metric of these people is 0.954 (95% CI 0.951–0.958) with a mean speed of 5.5 s per patient. The data for each patient are shown in Fig. S1.

Afterwards, we incorporated clinical factors and the spleen volume to build the spleen-based model. We used the least absolute shrinkage and selection operator (LASSO)-Cox algorithm

to select prognostic features and build the model in a list of spleen volume and 25 clinical and laboratory variables (Table 1 footnote and Supplementary Methods 1.3) from the training set. Moreover, 1 SE was considered as the criterion to select the regulation weight (λ) on the leave-one-out cross-validation of the training cohort in LASSO-Cox regression. Finally, the model directly used the nonzero-coefficient variables and their coefficients from LASSO to output a linear predictor (risk score) for each patient. A larger risk score indicates an increased risk of decompensation. The spleen-based model was trained using the training cohort and applied to each patient and tested in 2 external validation cohorts.

Associations of spleen volume with 2D spleen measurements, decompensation risk, and clinical characteristics

To investigate whether 2D parameters can accurately reflect the spleen volume, we also calculated the maximum 3D diameter, major axis length, and maximum 2D diameters in the axial, coronal, and sagittal planes of the spleen using the segmentation results (Supplementary Methods 1.4). The relationship between spleen volume and 2D parameters of the spleen was evaluated by using the Pearson correlation in all patients. Furthermore, we used restricted cubic splines with 4 knots to flexibly model and visualise the association of spleen volume with decompensation.

To assess the added predictive value of spleen volume, we built a clinical model using LASSO-Cox, including only clinical and laboratory variables in the training cohort. The clinical model would generate a benchmark of potential prognostic variables. The difference in including variables and their coefficients between the clinical and spleen-based models would display the added predictive effect of the spleen volume.

Model performance and validation

The spleen-based model was initially assessed in the training cohort and then validated in 2 independent external cohorts. The prognostic performance was evaluated using Harrell's concordance index (C-index), time-dependent receiver operating characteristic curves (ROCs), areas under the curve (AUCs) at 3 and 5 years, calibration curves, and a decision curve analysis in all of the cohorts.

For less than 5% misdiagnosis,[4,23] the high-risk individuals were identified by applying a cut-off, which was based on the 95% sensitivity point on the time-dependent ROC at 3 years only from the training cohort. Then, the threshold was applied to the validation cohorts for the external test. Kaplan–Meier graphs were plotted with the log-rank test in each cohort according to the 2 risk groups.

Comparisons with serum-based models

We compared the prognostic power of the spleen-based model with that of conventional serum-based models, namely using the Child–Pugh score, MELD, ALBI, FIB-4, and ALBI-FIB-4 scores (which are based on the C-index,[24] time-dependent AUC, and decision curve analysis) in the training and validation cohorts. The net reclassification improvement (NRI) and integrated discrimination improvement (IDI) values[25] were evaluated to quantify the incremental prognostic improvement. Owing to the limited number of individuals that were included in both the clinical models and spleen-based models, the validation groups were combined.

LSM and comparisons with Baveno VII criteria

We compared spleen volume between different liver stiffness intervals in individuals with liver stiffness according to Baveno VII to explore the relationship between spleen volume and liver stiffness. Meanwhile, we assessed the risk stratification performance by the spleen-based model and Baveno VII criteria (low risk: LSM <15 kPa and PLT >150 × 10^9/L; high risk: LSM ≥25 kPa; and medium risk: other).[1] In addition, we compared the differences in liver stiffness between the high- and low-risk groups identified by the spleen-based model to verify whether our model is consistent with the existing theories based on LSM.

Robustness assessments of features and model

To assess the robustness of features, we performed a sensitivity Cox regression analysis with only spleen volume, cholinesterase (CHE), and Hb on the completed cases in both training and test cohorts.

To assess the robustness of the spleen-based model, 3 different training and test datasets were randomly enrolled for patients from all centres at a ratio of 7:3. The models were retrained using the same variables but trained by different patients' combinations and were tested and compared with the original model.

Statistical analysis

We reported continuous variables as the mean (SD) or median (IQR) and categorical variables as n (%). Differences between groups were compared using Mann–Whitney *U* tests for 2 groups and Kruskal–Wallis 1-way ANOVA for >2 groups. The Dunn test was used for pairwise comparison and the Holm correction method for *p* values for multiple comparisons. The Kaplan–Meier method with the log-rank test was used to estimate the cumulative incidence of decompensation events and compare survival curves in patient characteristics description and risk stratification. A Pearson correlation was used to evaluate the relationship between the variables. Restricted cubic splines with 4 knots were used to flexibly model and visualise the association of spleen volume with decompensation.

The LASSO-Cox method was used to build the prognostic model. Individuals with missing variables in the final model were not included in the model assessment. The prognostic performance was evaluated using C-index, time-dependent ROC, calibration curves, and decision curve analysis in the training and validation cohorts. A high-sensitivity (95% sensitivity) cut-off point was extracted from time-dependent ROC in the training cohort and was applied to the validation cohorts. Median survival, hazard ratio (HR), and percentage decompensation at 3 and 5 years were calculated for each risk group and were reported in each cohort.

To quantify the model's incremental prognostic improvement, the developed model would be compared with conventional serum-based models based on the C-index (Student's *t* test),[24] time-dependent AUC, decision curve analysis, NRI, and IDI[25] from the same samples. The stratified analyses were performed on weight, height, age, and sex to assess the interaction effects on the model predictions.

A total of 73 individuals experienced decompensation events in a training cohort of 282 persons. About 7 prognostic variables would be able to be investigated using the 10:1 rule of thumb for

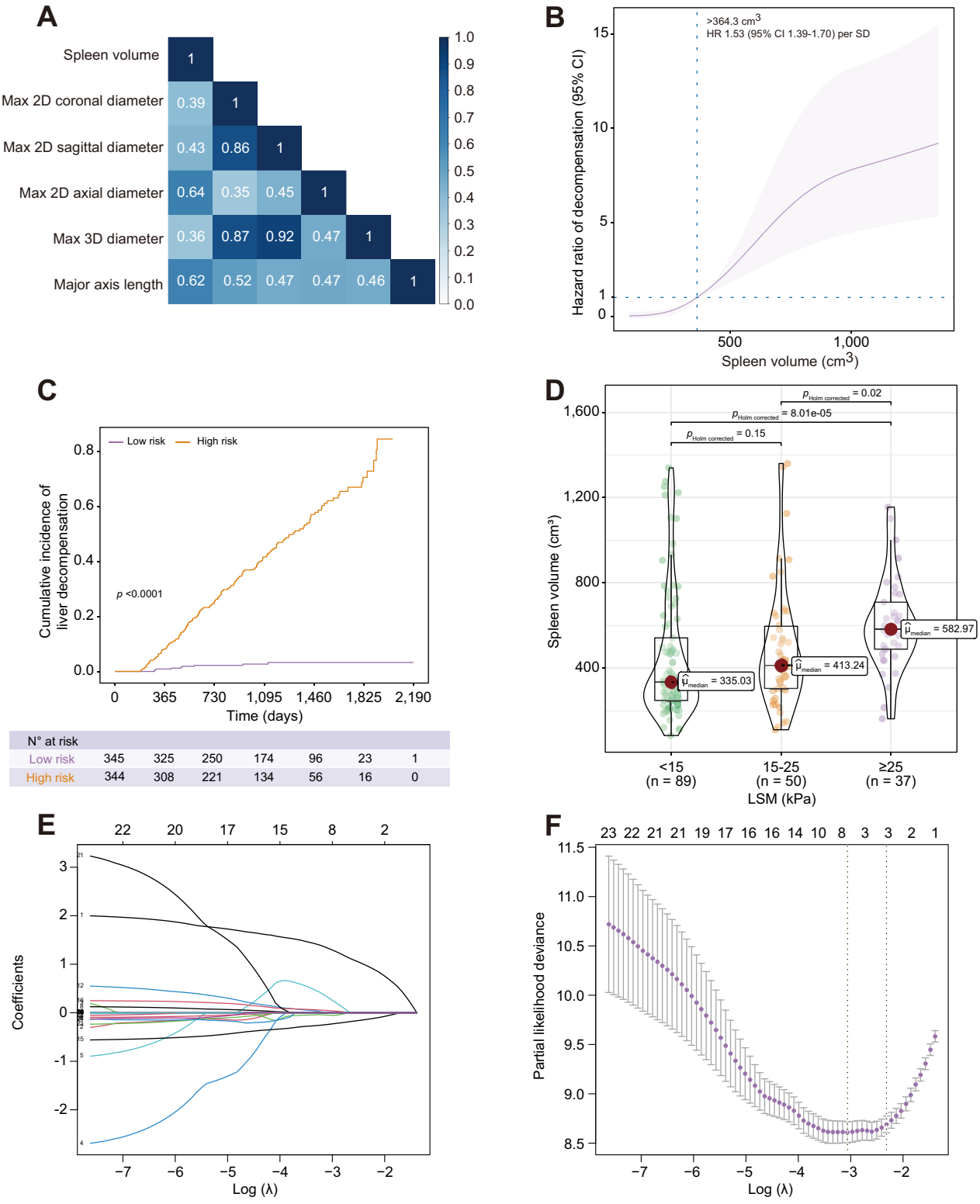

Fig. 3. Spleen volume analysis and model development. (A) Correlation matrix between spleen volume and the 2D parameters of the spleen (Pearson correlation, p <0.05 for all). (B) Restricted cubic splines for the association of spleen volume with decompensation ($p_{nonlinearity}$ <0.001). (C) Cumulative incidence of hepatic decompensation in all individuals defined by spleen volume >364.3 cm^3 (high risk) and ≤364.3 cm^3 (low risk; log-rank test, p <0.0001). (D) Spleen volume (cm^3) distribution in different liver stiffness sections and compared using Kruskal–Wallis 1-way ANOVA. According to Baveno VII, liver stiffness was divided by 15 and 25 kPa. (E and F) Spleen and clinical feature selection using the LASSO-Cox model. Number "1" in (E) is ln(spleen volume (cm^3)). We used the 1 SE of the minimum criteria to select variables (F, right vertical line), and finally, 3 of 26 nonzero coefficients features remained, namely spleen volume, cholinesterase (CHE), and Hb. 2D, 2-dimensional; 3D, 3-dimensional; CHE, cholinesterase; Hb, haemoglobin; LASSO, least absolute shrinkage and selection operator; HR, hazard ratio; LSM, liver stiffness measurement.

Table 2. Summary of C-index, median decompensation percentage, and hazard ratio of different risk groups in each cohort.

	C-index (95% CI)	Time-dependent AUC		Category	Number of patients (%)	Median decompensation-free survival (years)	Decompensation at 3 years n (%)	Decompensation at 5 years n (%)	Hazard ratio (95% CI)
		3-year	5-year						
Training cohort	0.84 (0.79–0.88)	0.84	0.90	Low risk	99 (46.3)	Not reached	1 (1)	1 (1)	7.3 (4.2–12.8) (p <0.001)
				High risk	115 (53.7)	4.2	33 (28.7)	48 (41.7)	
External validation cohort 1	0.87 (0.79–0.94)	0.89	0.91	Low risk	41 (51.9)	Not reached	0 (0)	0 (0)	5.8 (3.9–8.6) (p <0.001)
				High risk	38 (48.1)	3.5	14 (36.8)	19 (50)	
External validation cohort 2	0.84 (0.80–0.87)	0.89	0.91	Low risk	109 (36.6)	Not reached	1 (0.9)	2 (1.8)	
				High risk	189 (63.4)	3.8	69 (36.5)	81 (42.9)	

Hazard ratios, 95% CIs, and p values were estimated using the log-rank approach.
AUC, area under the curve.

prediction models. Then, 95% CIs were reported for the C-index, HR, IDI, and NRI. Statistical significance was set at a 2-tailed p value of <0.05.

The statistical analysis was conducted in R software (version 4.1.0; https://www.r-project.org R Foundation for Statistical Computing, Vienna, Austria). R codes are available on GitHub (https://github.com/vanziaa/Spleen_volume), and the main R packages used are in Supplementary Methods 1.5.

Results

Patient characteristics

Individuals (689) were enrolled in this study between 2016 and 2020, as shown in Fig. 1. A total of 441/689 (64%) persons were male, and the median age was 54 years (IQR 47–64 years). The median length of follow-up was 37.6 months (IQR 21.1–52.1 months) for the training cohort and 31 months (IQR 19.8–43.3 months) for the validation cohorts. The decompensation proportion had no significant difference between the 2 cohorts (log-rank test, p = 0.28). The baseline characteristics of the training and validation cohorts are described in Table 1.

The decompensation rate at 3 years was 23%, with an overall decompensation rate of 26%. The acute decompensation rate was 10%. The most common decompensation event was ascites (113/184 [61%]), followed by variceal bleeding (57/184 [31%]) and hepatic encephalopathy (14/184 [8%]). Two persons died after developing severe acute decompensation. A total of 123 people with HBV definitely achieved sustained virological responses at baseline.

Spleen volume at baseline

At baseline, the median spleen volume was 354.2 cm^3 (IQR 216.2–567.0 cm^3) in training and 371.6 cm^3 (IQR 228.9–576.3 cm^3) in validation individuals, without a noticeable difference between the training and validation cohorts (p = 0.80). A moderate correlation was observed between spleen volume and maximum 2D diameters in the axial plane (Pearson r = 0.64, p <0.001), followed by the major axis length (r = 0.62, p <0.001), whereas the other 2D parameters had a weak correlation with spleen volume (Fig. 3A).

The baseline spleen volume was markedly larger in individuals who developed first decompensation (median, 413.8 *vs.* 302.1 cm^3 in those remaining compensated; p <0.001). In Fig. 3B, the relationship between spleen volume and decompensation in all individuals was visualised using restricted cubic splines. The risk of decompensation was relatively low until the spleen enlargement was 364.3 cm^3, which was followed by a rapid increase ($p_{nonlinearity}$ <0.001). For a splenic volume above 364.3 cm^3, the HR per SD of higher spleen volume was 1.53 (95% CI 1.39–1.70), and a significantly higher risk of decompensation was observed in the larger spleen volume group (Fig. 3C). Therefore, spleen volume was considered a predictor for liver decompensation for this analysis.

Model development

Spleen volume was negatively correlated with PLT (r = −0.45, p <0.001), followed by FIB-4 (r = −0.42, p <0.001), whereas other clinical indicators were less correlated (Fig. S2A). For the nonlinearity relationship between spleen volume and decompensation ($p_{nonlinearity}$ <0.001), the natural logarithm of spleen volume ($p_{nonlinearity}$ = 0.02) and all of the clinical variables

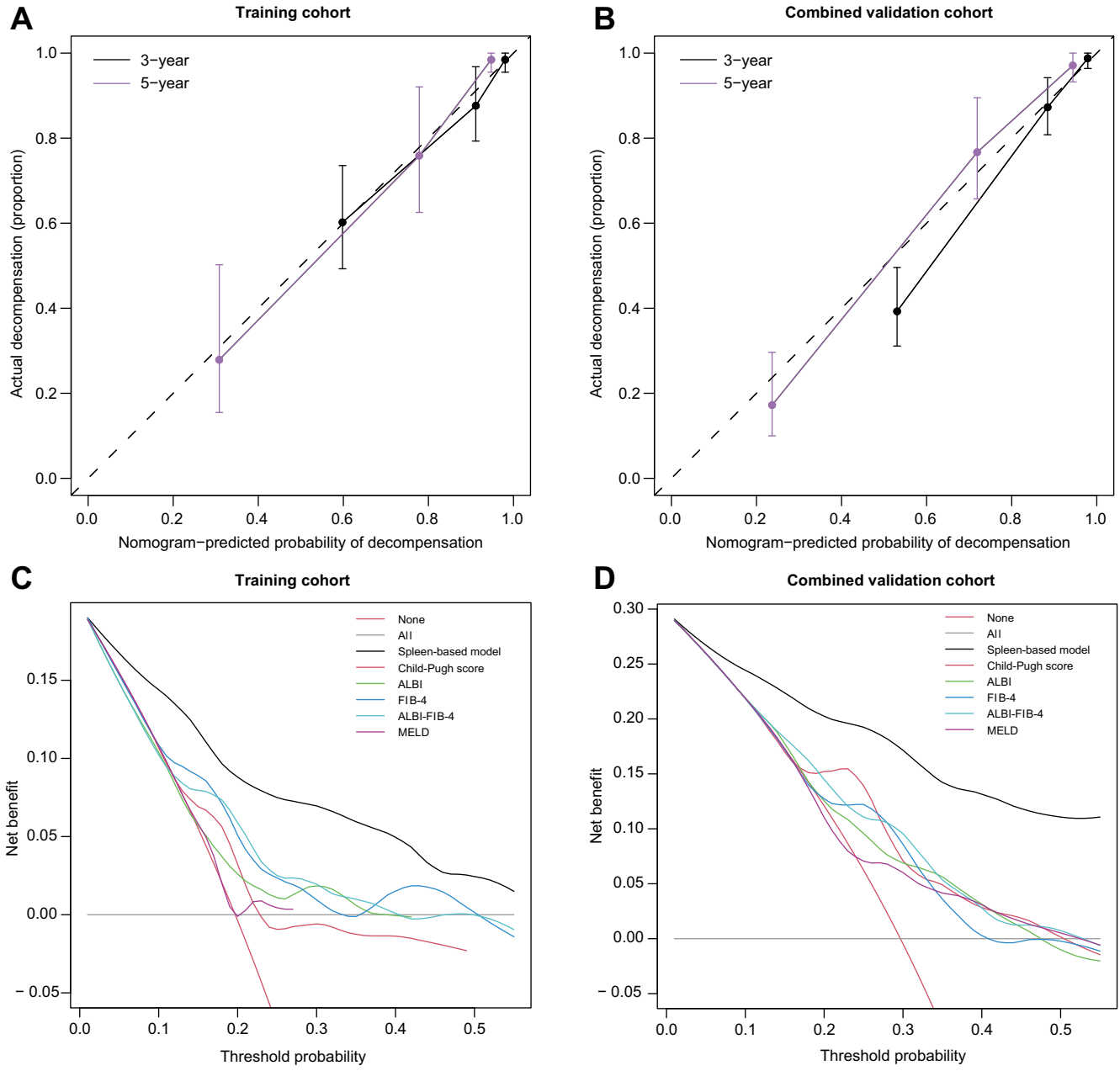

Fig. 4. Calibration curves and decision curve comparison in the training and validation cohorts. (A and B) The calibration curves for the spleen-based model at 3 and 5 years in the training (A) and validation cohorts (validation cohorts 1 and 2 were combined in B). (C and D) The decision curves for the spleen-based model and other conventional models in the training (C) and combined validation cohort (D). ALBI, albumin–bilirubin; FIB-4, Fibrosis-4; MELD, model for end-stage liver disease.

(A total of 26 variables) were incorporated into a LASSO-Cox regression to build the spleen-based model (Fig. 3E and 3F). The spleen volume strongly replaced some traditional markers, including PLT, alkaline phosphatase (ALP), and FIB-4 (Table S2).

Spleen volume (cm^3, natural logarithm), CHE, and Hb remained to form the model (risk score in Table S2). Coefficient changes are presented in Table S2 and Fig. S2B and C. A set of 591 individuals with spleen volume, CHE, and Hb were enrolled in model validation in the next step.

Model performance

The spleen-based model indicated good prognostic performance for all-cause decompensation with a C-index of 0.84 (95% CI 0.79–0.88) in the training cohort and C-indexes of 0.87 (95% CI 0.79–0.94) in validation cohort 1 and 0.84 (95% CI 0.80–0.87) in validation cohort 2 (Table 2). The AUCs at 3 and 5 years also confirmed a favourable prognostic accuracy (Table 2 and Fig. S3). The subgroup analysis of acute decompensation further showed good performance (Table S3).

Table 3. Comparison between spleen-based model and other scores for all-cause decompensation.

Model	C-index (95% CI)	Time-dependent AUC		IDI (95% CI)	*p* value (IDI)	NRI (95% CI)	*p* value (NRI)
		3 years	5 years				
Training cohort							
Spleen-based model	0.84 (0.79–0.88)*	0.84	0.9	Benchmark		Benchmark	
Child–Pugh score	0.68 (0.58–0.79)†	0.59	0.59	0.43 (0.25–0.58)	0.009	0.73 (0.46–0.95)	0.01
MELD	0.5 (0.41–0.59)†	0.56	0.38	0.50 (0.30–0.65)	0.01	0.73 (0.39–0.94)	0.009
ALBI	0.61 (0.52–0.7)†	0.55	0.6	0.38 (0.23–0.51)	0.007	0.66 (0.31–0.85)	0.01
FIB-4	0.73 (0.66–0.8)†	0.71	0.77	0.34 (0.19–0.5)	0.003	0.64 (0.24–0.84)	0.02
ALBI-FIB4	0.7 (0.62–0.78)†	0.66	0.7	0.34 (0.18–0.47)	0.005	0.64 (0.29–0.83)	0.02
External validation cohort							
Spleen-based model	0.84 (0.81–0.87)*	0.89	0.91	Benchmark		Benchmark	
Child–Pugh score	0.72 (0.66–0.78)†	0.71	0.7	0.28 (0.14–0.43)	0.007	0.45 (0.09–0.78)	0.01
MELD	0.62 (0.56–0.68)†	0.63	0.63	0.32 (0.15–0.48)	0.01	0.43 (0.06–0.73)	0.03
ALBI	0.68 (0.62–0.73)†	0.69	0.73	0.28 (0.13–0.42)	0.006	0.44 (0.13–0.73)	0.02
FIB-4	0.68 (0.63–0.74)†	0.72	0.81	0.29 (0.11–0.46)	0.02	0.52 (0.21–0.8)	0.02
ALBI-FIB4	0.7 (0.65–0.75)†	0.72	0.79	0.24 (0.09–0.4)	0.01	0.5 (0.09–0.72)	0.02

p values and 95% CIs and for IDI and NRI were estimated using perturbation resampling (1,000 iterations).
ALBI, albumin–bilirubin; AUC, area under the curve; FIB-4, Fibrosis-4; IDI, integrated discrimination improvement; MELD, model for end-stage liver disease; NRI, net reclassification improvement.
* Reference of C-index comparison.
† *p* values <0.001 for each model compared with the spleen-based model from the same samples using Student's *t* test.

The calibration curves (Fig. 4A and B) for the spleen-based model at 3 and 5 years showed good agreement between estimations and clinical outcomes in the development and validation cohorts. These results confirmed the high prognostic accuracy of the model.

Stratified analyses were performed by weight, height, age (≤mean and >mean), and sex. There were no significant interactions in any of the subgroups ($p_{interaction}$ >0.05 for all), which confirmed that the model was not affected by height, weight, age, or sex (Table S4).

The incremental value of the spleen-based model

The C-index and AUCs at 3 and 5 years for the spleen-based model and the conventional serum-based models in the training and combined validation cohorts are listed in Table 3 (all decompensation) and Table S3 (acute decompensation), by the limited number of patients having the clinical models and spleen-based models at the same time. Relative to the serum-based models, the spleen-based model showed better performance in both the training (C-index was 0.826–0.833) and validation cohorts (C-index was 0.831–0.841) on the same shared patients. NRI and IDI results confirmed that the spleen model exhibited higher accuracy and significant improvement in the classification accuracy for decompensation (Table 3).

The decision curve analysis demonstrated that the spleen-based model provided good clinical performance across the range of reasonable threshold probabilities compared with other models in the training and validation cohorts (Fig. 4C and D). These results revealed that the spleen-based model had an incremental value for personalised decompensation prediction.

Risk stratification

With the use of 4.4 as the cut-off from the 95% sensitivity at 3 years only from the training cohort, people were classified into high- and low-risk groups. The time-to-event curves confirmed a clear separation in both the all-cause decompensation and acute decompensation between the low- and high-risk groups in all 3 cohorts (p <0.001, Fig. 5 and Fig. S4A and C; p = 0.009, Fig. S4B), with HRs of 7.3 (95% CI 4.2–12.8) in the training cohort and 5.8 (95% CI 3.9–8.6) in the 2 validation cohorts when evaluating the low-risk group *vs.* the high-risk group (Table 2).

One of 99 (1%) individuals in the training cohort and 1 of 150 (<1%) individuals in the validation cohorts in the low-risk group, identified by the spleen model, developed decompensation events within 3 years. The details of individuals who reached decompensation events are described in Table 2 and Fig. 5A and C. These results suggested that the model had good risk stratification ability.

LSM and comparisons with Baveno VII criteria

In a subgroup including 176 individuals with LSM in validation cohort 2, baseline spleen volume was significantly larger in individuals with LSM ≥25 kPa than in individuals with LSM <15 and 15∼25 kPa (*i.e.* median: 583.0 *vs.* 335.0 cm^3, and 583.0 *vs.* 413.2 cm^3, pairwise comparison $P_{Holm\text{-}corrected}$ <0.05, as shown in Fig. 3D). Notably, we found higher LSM results in high-risk individuals identified by the model, an important predictive factor linked to decompensation (Fig. 5F), which explains why they face a higher risk of decompensation.

According to Baveno VII, a clear separation between the low-, middle-, and-high-risk groups was observed in the criteria in Fig. 5. People in the low-risk group by the Baveno VII criteria, including LSM and PLT, did not develop any decompensation events during follow-up. However, the HR of reaching decompensation was 1.9 (95% CI 0.9–3.8, p = 0.07) between the middle- and high-risk groups according to Baveno VII. The spleen-based model identified more low-risk individuals than the Baveno VII criteria (60/176 [34.1%] *vs.* 18/176 [10.2%]) with 1 misclassification (1/60 [1.7%]). A similar risk stratification result by the Baveno VI criteria is shown in Fig. S5. The competitive risk stratification results suggested that the model could be a potential alternative when LSM is unavailable.

Robustness assessments of features and model

The sensitivity Cox regression analysis showed that the 3 variables remained significant related to the composite endpoint in the training and combined test (external validation) cohorts (Table S5). In addition, the trend of HR is consistent with the

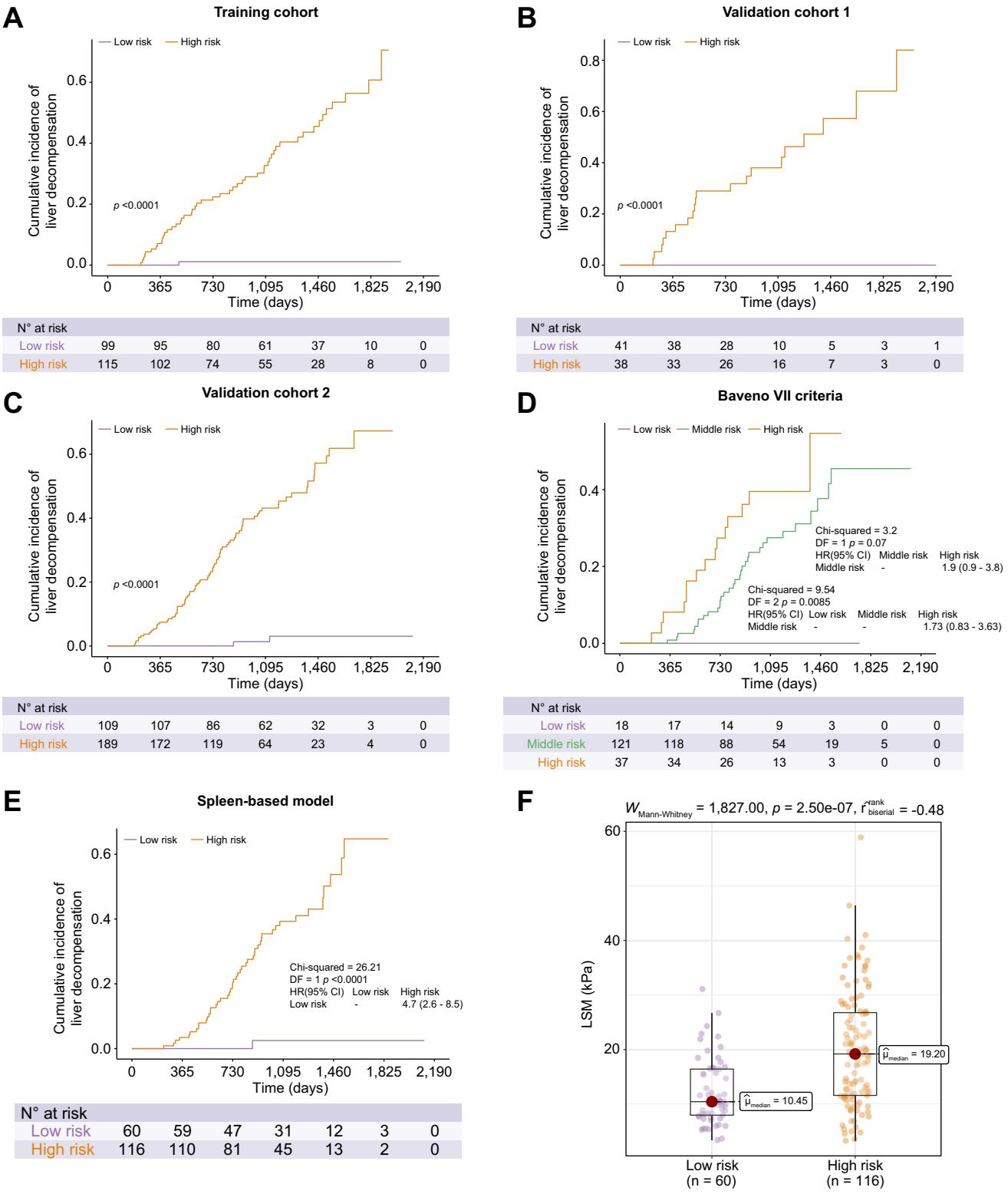

Fig. 5. Risk stratification by the spleen-based model. (A–C) Cumulative incidence of all-cause hepatic decompensation in the training and validation cohorts defined by the spleen-based model. (D and E) Cumulative incidence of all-cause hepatic decompensation by Baveno VII and the spleen-based model in the validation cohorts. (A)–(E) were reported using the Kaplan–Meier method with the log-rank test (A–C and E p <0.0001; D high-risk *vs.* middle-risk group p = 0.07; high-risk *vs.* middle- and low-risk group p = 0.0085). (F) LSM between high-risk and low-risk individuals identified by the model (Mann–Whitney U test, p <0.05). DF, degree of freedom; HR, hazard ratio; LSM, liver stiffness measurement.

model in our study that a larger spleen volume implies a higher risk of decompensation, whereas CHE and Hb are on the contrary.

After retraining and testing, there was no variation in the C-indexes in different training and test datasets (Fig. S6). These experiments illustrate the robustness of the model and features selected by cross-validation.

Discussion

Decompensation leads to increased mortality risk, and NITs that are used to stratify the liver decompensation risk remain unmet. In this study, we described the relationship between the spleen volume and the increase in decompensation risk. We built an artificial intelligence-driven spleen-based model and validated it using external test cohorts. The proposed model was able to predict decompensation (C-index ≥0.84) independently of the aetiology, better than the traditional serum-based models (C-index, NRI, and IDI test p <0.05 for all cohorts) in both training and external validation cohorts, suggesting its good reliability and reproducibility. The model could predict individual decompensation risk (log-rank test, p <0.05). Specifically, individuals in the low-risk group had a negligible 3-year risk (≤1%) of decompensation. The similar performance of the proposed model compared with the Baveno VII criteria suggested its potential clinical applicability in diverse healthcare settings where HVPG/LSM are not available.

Our sample consisted of 689 persons with compensated cirrhosis, with 88% of them having a Child–Pugh score of ≤7, and the median MELD score of the patients was <7 at baseline. Our study had a similar median follow-up time of 37.6 months (IQR 21.1–52.1 months) and decompensation rate at 3 years of 23% compared with previous studies.[10,13,21,26,27] With more than 2 billion people infected with chronic hepatitis as estimated by the World Health Organization (WHO), our findings might be generalised to patients in other countries, especially in Asian and African regions, given the appropriate follow-up and decompensation rate.[28]

Herein, we described the spleen volume enlargement in people with cirrhosis. Previous studies have provided us with population-based reference intervals of approximately 81.1–322.0 cm^3 for the spleen volume in healthy donors, and these intervals allow us to independently assess the size of the spleen.[14] We observed a larger spleen volume (median 413.8 cm^3) in decompensated individuals at baseline, which exceeds the upper limit. We also observed a nonlinear increase in the decompensation risk starting at 364.3 cm^3 in all patient cohorts. However, Yoo *et al.*[12] proposed a cut-off of 656.9 ml for spleen volume for decompensation, which is larger than our observation, especially from the LSM perspective. Median spleen volumes were 413 and 583 cm^3 when LSM is larger than 15 and 25 kPa, respectively, which means relatively higher risks of decompensation independent of the aetiology and ruling in CSPH.[1] A higher threshold would underestimate the decompensation risk in individuals with smaller spleen volumes.

The ability of the spleen volume to accurately predict decompensation confirms its prognostic value, showing better performance than serum indicators. When spleen volume was entered into the model, the importance for decompensation of ALP, PLT, and FIB-4 was obliterated by the spleen volume, which suggests an added predictive value from the spleen. The decreased CHE and Hb levels reflect decreased liver function and hypersplenism. The use of these factors can improve decompensation risk apart from structural alterations.[13,29,30] Combining the above 2 points, the spleen-based model outperformed the traditional serum-based models. Aetiology was initially sieved out during model building, implying it was less important,[27] and the model could be applied to different aetiologies. Additionally, ALBI and ALBI-FIB4 scores were also better predictors than the Child–Pugh score and MELD score in our study, which is consistent with a previously reported study.[22]

However, the prognostic role of liver volume, as compared with spleen volume, in the transition from compensation to decompensation does not appear to be clear. There was no difference in the liver volume in decompensated individuals as compared with healthy participants and compensated persons.[10] The tendency for the liver volume to increase or decrease during cirrhosis was not apparent.[14] Liver volume was also reported to have a low diagnostic capability for high-risk varix[11] and CSPH.[18] Therefore, the liver volume was not analysed.

We also assessed the Baveno VII criteria for risk stratification in a subgroup of the validation group. The Baveno VII criteria could be highly effective in identifying low-risk individuals by ruling out CSPH. However, compared with high-risk individuals (ruled in CSPH), middle-risk group individuals seem to have the same decompensation risk. There were differences between the EASL guidelines[4] and the Baveno VII criteria also.[1] Liu *et al.*[26] proposed a more detailed method for predicting decompensation. Further research is required for the Baveno VII criteria.

The strength of our study was that individuals could be effectively stratified into low- and high-risk groups similar to the Baveno VII criteria, where the low-risk group had a negligible decompensation risk (≤1%) in both training and external validation cohorts. Our spleen model achieves a competitive prognostic ability, which is similar to that of LSM or spleen stiffness measurement reported,[26,31,32] and the model outperformed the accessible serum-based models.[22] A higher LSM was observed in the high-risk group identified by the model, which explains why they face a higher risk of decompensation. Compared with liver stiffness, the spleen volume could be easily obtained by CT and MRI using a public segmentation algorithm. Because the model uses easy, non-invasive, and repeatable variables, it offers a means for clinicians to select personalised prophylactic strategies and assess risks repeatedly[1] without additional time and efforts in diverse healthcare settings where HVPG and LSM are not available. The decision curve analysis suggested that patients would benefit from the spleen-based model.

Our study has some limitations to be considered. First, there is an inherent bias that resulted from the retrospective study design, although an external validation was conducted to test the reliability. Second, there are concerns regarding the ionising radiation from the CT scans. Spleen segmentation on MRI is worth evaluating. Finally, virus-related cirrhosis remained the predominant aetiology in our study, although aetiologies have been enrolled in model building and were sieved out. The model would be further validated in other aetiologies.

In conclusion, we developed a spleen-based clinical features-combined model that effectively predicted decompensation in people with compensated cirrhosis. Our model provides a user-friendly tool to help select personalised prophylactic strategies in individuals with cirrhosis when HVPG and LSM are not available.

Abbreviations

2D, 2-dimensional; 3D, 3-dimensional; ALBI, albumin–bilirubin; ALP, alkaline phosphatase; AUC, area under the curve; CHE, cholinesterase; C-index, concordance index; CSPH, clinically significant portal hypertension; CT, computed tomography; FCN, fully convolutional network; FIB-4, Fibrosis-4; Hb, haemoglobin; HR, hazard ratio; HVPG, hepatic venous pressure gradient; IDI, integrated discrimination improvement; LASSO, least absolute shrinkage and selection operator; LSM, liver stiffness measurement; MELD, model for end-stage liver disease; MRI, magnetic resonance imaging; NIT, non-invasive tool; NRI, net reclassification improvement; PLT, platelet; ROC, receiver operating characteristic curve; TIPS, transjugular intrahepatic portosystemic shunt; WHO, World Health Organization.

Financial support

This research was supported by the National Natural Science Foundation of China (NSFC; Nos. 81830053, 82001779, and 92059202), the Key Research and Development Program of Jiangsu Province (BE2020717), and the Nature Science Foundation of Jiangsu Province (No. BK20200368).

Conflicts of interest

There are no conflicts of interest to declare.

Please refer to the accompanying ICMJE disclosure forms for further details.

Authors' contributions

Conception and design of the work: SHJ, QY.
Patient recruitment: SHJ, CJX, JY.
Acquisition of data: QYL, YL, ZMD, JYZ, YFL, SH.
Analysis or interpretation of data: CX, CL, QY, YFH.
Method development: QY.
Supervision: TYT, CL, CQL, YS, XLQ.
Drafting of the manuscript: QY.
Revision of the manuscript: YCW, SHJ, XLQ, CL, SH, YS, TYT.
Critical review and final approval of the manuscript: All authors.
The corresponding author attests that all listed authors meet authorship criteria and that no others meeting the criteria have been omitted.

Data availability statement

The codes in the current study are available on GitHub (https://github.com/vanziaa/Spleen_volume). The datasets in this study are not publicly available but are available from the corresponding author on reasonable request.

Acknowledgements

We would like to thank Mr. Ben Zhao, Mr. Yin Gao, and Ms. Boyue Cao for their contribution in model testing. Further, we would like to thank Prof. Yongyue Wei, Department of Biostatistics, Nanjing Medical University, for the professional statistical and methodological consulting.

Supplementary data

Supplementary data to this article can be found online at https://doi.org/10.1016/j.jhepr.2022.100575.

References

Author names in bold designate shared co-first authorship

[1] de Franchis R, Bosch J, Garcia-Tsao G, Reiberger T, Ripoll C, Baveno VII Faculty. Baveno VII – renewing consensus in portal hypertension: report of the Baveno VII Consensus Workshop: personalized care in portal hypertension. J Hepatol 2022;76:959–974.

[2] D'Amico G, Bernardi M, Angeli P. Towards a new definition of decompensated cirrhosis. J Hepatol 2022;76:202–207.

[3] Garcia-Tsao G, Abraldes JG, Berzigotti A, Bosch J. Portal hypertensive bleeding in cirrhosis: risk stratification, diagnosis, and management: 2016 practice guidance by the American Association for the study of liver diseases. Hepatology 2017;65:310–335.

[4] Berzigotti A, Tsochatzis E, Boursier J, Castera L, Cazzagon N, Friedrich-Rust M, et al. EASL Clinical Practice Guidelines on non-invasive tests for evaluation of liver disease severity and prognosis – 2021 update. J Hepatol 2021;75:659–689.

[5] Giannini E, Botta F, Borro P, Risso D, Romagnoli P, Fasoli A, et al. Platelet count/spleen diameter ratio: proposal and validation of a non-invasive parameter to predict the presence of oesophageal varices in patients with liver cirrhosis. Gut 2003;52:1200–1205.

[6] Berzigotti A, Zappoli P, Magalotti D, Tiani C, Rossi V, Zoli M. Spleen enlargement on follow-up evaluation: a noninvasive predictor of complications of portal hypertension in cirrhosis. Clin Gastroenterol Hepatol 2008;6:1129–1134.

[7] Berzigotti A, Seijo S, Arena U, Abraldes JG, Vizzutti F, García-Pagán JC, et al. Elastography, spleen size, and platelet count identify portal hypertension in patients with compensated cirrhosis. Gastroenterology 2013;144:102–111.e1.

[8] Gracia-Sancho J, Marrone G, Fernández-Iglesias A. Hepatic microcirculation and mechanisms of portal hypertension. Nat Rev Gastroenterol Hepatol 2019;16:221–234.

[9] Abraldes JG, Bureau C, Stefanescu H, Augustin S, Ney M, Blasco H, et al. Noninvasive tools and risk of clinically significant portal hypertension and varices in compensated cirrhosis: the "Anticipate" study. Hepatology 2016;64:2173–2184.

[10] Bradley CR, Cox EF, Scott RA, James MW, Kaye P, Aithal GP, et al. Multiorgan assessment of compensated cirrhosis patients using quantitative magnetic resonance imaging. J Hepatol 2018;69:1015–1024.

[11] Lee C, Lee SS, Choi W-M, Kim KM, Sung YS, Lee S, et al. An index based on deep learning–measured spleen volume on CT for the assessment of high-risk varix in B-viral compensated cirrhosis. Eur Radiol 2021;31:3355–3365.

[12] **Yoo J**, **Kim SW**, Lee DH, Bae JS, Cho EJ. Prognostic role of spleen volume measurement using computed tomography in patients with compensated chronic liver disease from hepatitis B viral infection. Eur Radiol 2021;31:1432–1442.

[13] D'Amico G, Garcia-Tsao G, Pagliaro L. Natural history and prognostic indicators of survival in cirrhosis: a systematic review of 118 studies. J Hepatol 2006;44:217–231.

[14] **Kim DW**, **Ha J**, Lee SS, Kwon JH, Kim NY, Sung YS, et al. Population-based and personalized reference intervals for liver and spleen volumes in healthy individuals and those with viral hepatitis. Radiology 2021;301:339–347.

[15] Perez AA, Noe-Kim V, Lubner MG, Graffy PM, Garrett JW, Elton DC, et al. Deep learning CT-based quantitative visualization tool for liver volume estimation: defining normal and hepatomegaly. Radiology 2021;302:336–342.

[16] Shung DL, Au B, Taylor RA, Tay JK, Laursen SB, Stanley AJ, et al. Validation of a machine learning model that outperforms clinical risk scoring systems for upper gastrointestinal bleeding. Gastroenterology 2020;158:160–167.

[17] Dong TS, Kalani A, Aby ES, Le L, Luu K, Hauer M, et al. Machine learning-based development and validation of a scoring system for screening high-risk esophageal varices. Clin Gastroenterol Hepatol 2019;17:1894–1901.e1.

[18] **Yu Q**, **Huang Y**, **Li X**, **Pavlides M**, Liu D, Luo H, et al. An imaging-based artificial intelligence model for non-invasive grading of hepatic venous pressure gradient in cirrhotic portal hypertension. Cell Rep Med 2022;3:100563.

[19] Kwon JH, Lee SS, Yoon JS, Suk H-I, Sung YS, Kim HS, et al. Liver-to-spleen volume ratio automatically measured on CT predicts decompensation in patients with B viral compensated cirrhosis. Korean J Radiol 2021;22:1985–1995.

[20] de Franchis R, Baveno VI Faculty. Expanding consensus in portal hypertension: report of the Baveno VI Consensus Workshop: stratifying risk and individualizing care for portal hypertension. J Hepatol 2015;63:743–752.

[21] Mendoza Y, Cocciolillo S, Murgia G, Chen T, Margini C, Sebastiani G, et al. Noninvasive markers of portal hypertension detect decompensation in overweight or obese patients with compensated advanced chronic liver disease. Clin Gastroenterol Hepatol 2020;18:3017–3025.e6.

[22] Guha IN, Harris R, Berhane S, Dillon A, Coffey L, James MW, et al. Validation of a model for identification of patients with compensated cirrhosis at high risk of decompensation. Clin Gastroenterol Hepatol 2019;17:2330–2338.e1.

[23] Stafylidou M, Paschos P, Katsoula A, Malandris K, Ioakim K, Bekiari E, et al. Performance of Baveno VI and Expanded Baveno VI criteria for excluding high-risk varices in patients with chronic liver diseases: a systematic review and meta-analysis. Clin Gastroenterol Hepatol 2019;17:1744–1755.e11.

[24] Schröder MS, Culhane AC, Quackenbush J, Haibe-Kains B. survcomp: an R/Bioconductor package for performance assessment and comparison of survival models. Bioinformatics 2011;27:3206–3208.
[25] Uno H, Tian L, Cai T, Kohane IS, Wei LJ. A unified inference procedure for a class of measures to assess improvement in risk prediction systems with survival data. Stat Med 2013;32:2430–2442.
[26] **Liu Y**, **Liu C**, **Li J**, Kim TH, Enomoto H, Qi X. Risk stratification of decompensation using liver stiffness and platelet counts in compensated advanced chronic liver disease (CHESS2102). J Hepatol 2022;76:248–250.
[27] D'Amico G, Perricone G. Prediction of decompensation in patients with compensated cirrhosis: does etiology matter? Curr Hepatol Rep 2019;18:144–156.
[28] Schmit N, Nayagam S, Thursz MR, Hallett TB. The global burden of chronic hepatitis B virus infection: comparison of country-level prevalence estimates from four research groups. Int J Epidemiol 2021;50:560–569.
[29] Santarpia L, Grandone I, Contaldo F, Pasanisi F. Butyrylcholinesterase as a prognostic marker: a review of the literature. J Cachexia Sarcopenia Muscle 2013;4:31–39.
[30] Sun X, Zhang A, Zhou T, Wang M, Chen Y, Zhou T, et al. Partial splenic embolization combined with endoscopic therapies and NSBB decreases the variceal rebleeding rate in cirrhosis patients with hypersplenism: a multicenter randomized controlled trial. Hepatol Int 2021;15:741–752.
[31] Colecchia A, Colli A, Casazza G, Mandolesi D, Schiumerini R, Reggiani LB, et al. Spleen stiffness measurement can predict clinical complications in compensated HCV-related cirrhosis: a prospective study. J Hepatol 2014;60:1158–1164.
[32] Robic MA, Procopet B, Métivier S, Péron JM, Selves J, Vinel JP, et al. Liver stiffness accurately predicts portal hypertension related complications in patients with chronic liver disease: a prospective study. J Hepatol 2011;55:1017–1024.